

Time-dependent Mechanical Behavior of Sweet Sorghum Stems

Seunghyun Lee¹, Omid Zargar¹, Carl Reiser¹, Qing Li², Anastasia Muliana¹, Scott A. Finlayson², Francisco E. Gomez^{3*}, and Matt Pharr^{1*}

¹Department of Mechanical Engineering, Texas A&M University

²Department of Soil and Crop Sciences, Faculty of Molecular and Environmental Plant Sciences, Texas A&M University

³University of Minnesota, Department of Agronomy and Plant Genetics, St. Paul, MN 55108, USA

Seunghyun Lee: **sel068@tamu.edu**

Omid Zargar: **ozargar@tamu.edu**

Carl Reiser: **creiserjr@tamu.edu**

Qing Li: **liqing@tamu.edu**

Anastasia Muliana: **amuliana@tamu.edu**

Scott A. Finlayson: **sfinlayson@tamu.edu**

*Francisco E. Gomez: **gomez225@umn.edu**

*Matt Pharr: **m-pharr@tamu.edu**

***Corresponding authors:**

E-mail: **m-pharr@tamu.edu, gomez225@umn.edu**

Abstract

Grasses represent the most productive and widely grown crop family across the globe but are susceptible to structural failure (lodging) during growth (e.g., from wind). The mechanisms that contribute to structural failure in grass stems are poorly understood due to a lack of systematic studies of their biomechanical behavior. To this end, this study examines the biomechanical properties of sweet sorghum (*Sorghum bicolor* (L.) Moench), focusing on the time-dependent behavior of the stems. Specifically, we conducted uniaxial compression tests under ramp and creep loading on pith and stem specimens of the sorghum cultivar Della. The tests demonstrated significantly nonlinear and time-dependent stress-strain behavior in all samples. We surmise that this behavior arises from a combination of poroelasticity due to migration of water through the plant and viscoelasticity due to rearrangement of macromolecular networks, such as cellulose microfibrils and lignin matrices. Overall, our measurements demonstrate that sorghum is not a simple reversible elastic material. As such, a complete understanding of the conditions that lead to stem lodging will require knowledge of sorghum's time-dependent biomechanical properties. Of practical importance, the time-dependent biomechanical properties of the stem influence its mechanical stability under various loading conditions during growth in the field (e.g., different wind speeds).

Keywords: Sorghum; Plants; Grasses; Stem lodging; Time/rate dependent response; Poroelasticity; Viscoelasticity.

1. Introduction

Grasses represent the most productive and widely grown crop family across the globe but are susceptible to structural failure (lodging) under mechanical loading [1, 2]. Stem lodging is a complex physical process that significantly reduces yield and quality in many of the cereal grasses (e.g., maize, rice, sorghum, wheat, etc.) [3]. Despite the economic significance of stem lodging, the mechanisms that contribute to structural failure in grass stems remain poorly understood. Quantitative methods including histochemical approaches, crushing strength measurements, rind penetrometry, and bending tests [4-12] have been applied to understand stem mechanical behavior. However, these methods may be insufficient to fully understand the deformation processes of stem structures [13, 14]. A better understanding of the parameters that produce the observed mechanical behavior of the cereal crops is critical to increase agricultural productivity as well as to provide fundamental knowledge of the mechanisms of stem lodging.

Sorghum (*Sorghum bicolor* (L.) Moench) is a useful model plant for studying stem structural failure because of its tremendous variation in height, stem thickness, tillering, stem composition, and end-use (food, forage, energy, fiber, building material, etc.), which is largely a result of disruptive selection [15-18]. This diversity in attributes provides a key advantage in terms of probing which factors most affect mechanical stability and structural failure in the cereal grasses. Sorghum, like all cereal crops, often mechanically fails because of wind pressure on the stem. This failure is a consequence of weak stems, which are either genetically inherited or caused by other factors such as pathogens [10, 19-21]. In response, plants have adapted unique stem anatomical, morphological, and mechanical properties to maintain structural integrity when subjected to dynamic loadings [22, 23]. As such, a complete time-dependent understanding of stem biomechanical properties is necessary to explain how plants can withstand stresses from wind. In turn, such understanding can be used by modelers to determine the mechanical stability of stems under various conditions (e.g., wind speed) as well as by plant breeders to potentially select for traits that confer greater mechanical stability (lodging resistant variants).

Previous studies have uncovered both genetic and spatial variation of sorghum mechanical properties, e.g., among genotypes and among both nodes and internodes at different positions [24-27]. A recent study implemented a three-point bending test and found that sorghum stems exhibited a significantly lower elastic modulus, strength, and flexural rigidity at the internodes, as compared to the nodes [25]. This spatial variation of properties may explain why sorghum stem lodging in the field nearly always occurs at the internodes, as has also been observed in other cereal crops [28, 29]. More lodging-resistant sorghum genotypes demonstrated stronger and more flexible (low flexural rigidity) stems with a lower elastic modulus [25]. Further investigation of stem failure, beyond simply determining the elastic modulus and ultimate strength is required to develop a better understanding of the mechanical behavior of grass stems. In particular, all studies to date treat sorghum stems as linearly elastic, which does not represent a realistic

mechanical response of the stems. Instead, plants are composite materials, consisting of various microstructural constituents at multiple length scales. At larger scales sorghum stems can be distinguished by their sclerenchymatous tissue (outer skin or epidermis and rind comprised of several sub-epidermal cell layers) and parenchymatous tissue (pith, consisting of vascular bundles and soft tissues). Green (living) sorghum has a high-water content, which may lead to pronounced time-dependent behavior associated with water viscosity. Mechanical pressures can cause water migration through the stem tissues, a time-dependent process known as poroelasticity. In addition to the high water content, the components of the plants themselves may exhibit viscoelastic behavior, a time-dependent response due to rearrangement of macromolecular networks, as they are based on polymeric building blocks (i.e. cellulose, hemicellulose, and lignin). Overall, the time-dependent behavior of sorghum stems can influence lodging, and it is important to characterize this behavior to gain a comprehensive understanding of sorghum's biomechanics. Thus, methods to quantify the mechanical behavior of stems requires tests that include a time component of testing [1].

The objective of this study was thus to uncover greater detail of the biomechanical behavior of sweet sorghum by investigating the more rigorous stress-strain behavior (i.e., beyond just the linear elastic regime) and time-dependent responses of stems and pith under uniaxial loading. To do so, we selected the sweet sorghum Della cultivar, which was grown in a greenhouse in a controlled environment. We conducted uniaxial compression tests under ramp and creep loading on pith and stem internodes. The results demonstrate that all of the tested samples of sorghum exhibit pronounced time-dependent mechanical responses. We conclude by detailing the ramifications of such effects in the context of stem lodging.

2. Materials and Methods

2.1. Plant material

The sorghum cultivar Della was used throughout. Della is a medium stature photoperiod insensitive sweet sorghum type with potential for use as a bioenergy feedstock due to its high sucrose content. Growth of the experimental material began April 13, 2019 in a greenhouse located at 30.6° N. Plants were grown in 19 L pots containing a fine sandy loam soil amended with 14-14-14 slow-release fertilizer. The temperature was 26-30 °C day/21-26 °C night, and the photoperiod was 14 h day/10 h night, with supplemental light provided by high pressure sodium lamps. Plants were harvested for mechanical testing at grain maturity, approximately 13 weeks after planting.

2.2. Sample preparation

Plants were harvested for mechanical testing by cutting the stems at the soil level. All sorghum samples were collected in the morning before temperatures increased and they lost water by

evapotranspiration, specifically between 8-10 AM. All tests were performed within 6 hours after cutting the internode from the plant. Samples from internodes 9 and 10 were used in all of the performed tests, randomly selected from among 10 replicate plants. For compression experiments, a precision saw (Buehler Isomet 1000 Precision saw) was used to cut the samples of pith and the entire stem to help ensure that their top and bottom surfaces were parallel (see the cross-section in **Figure 1**). Rigid test plates were used due to a lack of access to self-aligning platens (which would have been preferable). As such, some error may be introduced in the measurement, particularly at the very early stages of loading. However, our results do not indicate large fluctuations or variations at small loads, and as such, it appears that the use of the precision saw indeed helped mitigate these potential sources of error. The pith specimens were cut in a cylindrical shape from the center of the stem using steel tubes as the punch. The diameter of the pith and stem specimens was evaluated by measuring at three locations and taking an average value. **Figure 1** shows anatomical structures of Della sorghum. Differences in the structural morphology can influence the overall response of the stems. Measurements of the height (H) and diameter (D) were collected immediately after cutting using digital calipers. **Tables 1-6** summarize the dimensions of the tested samples. In selecting the aspect ratio of the test specimens, no specific ASTM standard exists for the vast majority of herbaceous plant stems, including sorghums[1], which are complicated composite structures. These materials are quite soft and compliant and as such are more susceptible to buckling than traditional engineering materials. To this end, we follow the sample preparation of Wright et al. (2005)[30] who have implemented an experimental method for compression testing of cellulosic feedstocks. In their approach, they use a height : diameter ratio of 1:1 to increase resistance to buckling.

2.3. Compression testing

Uniaxial compression tests were conducted on pith and stem specimens at room temperature using an Instron 5943 with a 1 kN load cell at a strain rate of 10%/min and 100%/min. The stress was calculated by dividing the force by the initial cross-sectional area, and the strain was calculated by dividing the displacement (cross-head displacement) by the initial height, i.e., all quantities represent nominal “engineering” values. The compression tests were performed up to failure of the specimens. All samples were oriented such that the axial direction of the plant was aligned to the direction of applied load. This orientation represents the primary direction of compression (and tension) that would occur during bending of the plants in the field. Due to their relatively small thickness, rind specimens were not suitable for compression tests and as such were not included in this study. In addition, compressive creep tests were conducted on pith and stem specimens to investigate time-dependent effects. Creep tests were performed for 1 hour at prescribed loads of 50% of strength as measured from the uniaxial compression tests of the piths and stems. The strength is defined by the peak in stress (before the specimens experienced

densification, as shown in **Figure 2**). In these creep tests, the specimens were initially ramped to the prescribed loads at a strain rate of 100%/min prior to the load hold. In all results, engineering stresses and strains were reported to evaluate the mechanical behaviors of the specimens.

2.4. Data analysis

Data was acquired through the Instron software (Bluehill® Universal 4.01) and processed in Microsoft Excel thereafter. To calculate the ‘elastic moduli’ of the specimens, the initial slopes under compression ramp tests were calculated from 0 to 0.5% (linear range) after implementing a standard toe correction method (following the procedure in ASTM D695). In materials that exhibit time-dependent responses (viscoelastic materials) the moduli of the materials cannot be determined by only measuring the slopes of the stress-strain curves, as these slopes change with the loading rates. Therefore, we will not refer to these slopes as elastic moduli of the specimens; instead, we will refer to them as the ‘initial slope’.

3. Results

3.1. Mechanical behavior under ramp compression tests

Uniaxial ramp compression tests at strain rates of 10%/min (slow) and 100%/min (fast) were performed to examine the mechanical behavior of the pith and stem of the Della genotype. **Figure 2** shows the engineering stress-strain responses under these conditions, which indicate that the full intact stems are stiffer and stronger than their corresponding piths, as expected. For the pith specimens, the calculated initial slopes from these tests were 25.8 (± 8.0) MPa for slow loading (10%/min) and 36.4 (± 7.5) MPa for fast loading (100%/min). For the entire stems, the calculated initial slopes were 130.1 (± 30.1) MPa for slow loading (10%/min) and 177.9 (± 50.5) MPa for fast loading (100%/min). Unpaired t-tests were used to identify differences between the initial slopes at the two loading rates of the stems and piths separately with the significance level at $p \leq 0.05$. These results demonstrated a strong influence of loading rate on the biomechanical properties of Della sorghum ($p = 0.0176$ for the stem and $p = 0.0061$ for the pith), thereby demonstrating its pronounced rate/time-dependent effects. As expected, the slower rate resulted in smaller slopes as more pronounced stress relaxation occurred due to the longer duration of loading. Deformation beyond the linear region further indicated strong rate effects. Under slow loading (10%/min), the pith showed a peak stress of 1.4 (± 0.5) MPa at a strain of 14.1 (± 6.7) %; under fast loading (100%/min), the pith showed a peak stress of 1.5 (± 0.3) MPa at a strain of 6.2 (± 1.4) %. The stress-strain responses of the pith specimens were highly nonlinear. Specifically, they demonstrated plateaus in stress between 14.1 (± 6.7) - 67.1 (± 5.9) % strain under slow loading (10%/min) and 6.2 (± 1.4) - 66.9 (± 6.6) % strain under fast loading (100%/min). These plateaus were followed by a rapid rise in stress at both loading rates. We surmise that this nonlinear deformation arose from continuous collapse of the cell walls (i.e., crushing), followed by

densification at a relatively large strain. Evidence of water loss from the pith was observed near the sample on the compression platen after testing. Water drained from the pith specimens very soon after loading and continued as compressive loads increased.

Both the stem and pith of Della showed qualitatively similar mechanical behavior, but with the stems demonstrating higher strengths (**Figure 2**). Specifically, under slow loading (10%/min), the stems showed a peak stress of $3.3 (\pm 0.3)$ MPa at a strain of $7.4 (\pm 1.8)$ %; under fast loading (100%/min), the stems showed a peak stress $4.0 (\pm 0.6)$ MPa at a strain of $5.9 (\pm 1.4)$ %. The stress-strain responses of the stem specimens were again highly nonlinear. Specifically, they demonstrated plateaus in stress between $7.4 (\pm 1.8)$ - $78.4 (\pm 4.3)$ % strain under slow loading (10%/min) and $5.9 (\pm 1.4)$ - $75.7 (\pm 4.1)$ % strain under fast loading (100%/min). These plateaus were followed by a rapid rise in stress at both loading rates.

The ultimate failure of the stems involved splitting between the rind and pith, followed by buckling and separation of the outer rind layer. For the pith specimen itself, failure likely involved breaking the vascular bundles and/or splitting the pith parenchyma accompanied by simultaneous water drainage of the sample (**Figures 1b and 1c**). Videos of representative tests are provided in **Videos 1-4**. **Videos 1 and 2** show a uniaxial ramp compression test at a strain rate of 10%/min (slow) of a stem and pith specimen, respectively, playing at 30x faster than real time. **Videos 3 and 4** show a uniaxial ramp compression test at a strain rate of 100%/min (fast) of a stem and pith specimen, respectively, playing at 3x faster than real time. Rind splitting and water drainage observed in Videos 1-4 indicate that irreversible deformation occurs in the non-linear regime of the stress-strain response in both the pith and stem. For instance, rind splitting near the bottom of the stem begins at around 3 seconds into Video 1. This rind splitting is not recoverable, and as such, will produce irreversible deformation. Time correlating with the stress-strain response in Figure 2 indicates highly nonlinear behavior beyond this point.

3.2. Mechanical response under compression creep loading

Stem failure in sorghum depends not only on the magnitude of loading but also on the rate and duration of loading [1]. Variations in these parameters are typical of the way that the crop experiences wind loading in the field. Therefore, it is critical to determine both the quasi-static and dynamic mechanical properties of sorghum, which requires characterizing time-dependent properties. To this end, we have selected creep tests as they are particularly conducive to determining viscoelastic material parameters, e.g., for use in future modeling studies. **Figure 3** shows representative plots from creep tests for pith and stem specimens under compression at $\sim 50\%$ of the strength as measured from compression ramp tests (i.e., from **Figure 2**). For the Della pith, the strain increased to $4.2 (\pm 0.7)$ % during a ramp loading at strain rate of 100%/min, followed by a continuous evolution to $9.6 (\pm 0.8)$ % after 1 hour under a constant load (**Figure 3a**). For the Della stem, the strain increased to $3.5 (\pm 1.0)$ % from a ramp loading at strain rate of 100%/min,

followed by a continuous slow evolution to 5.0 (± 1.2) % after 1 hour under a constant load (**Figure 3b**). Although the specific values of the strains in these tests varied, which may have depended on the characteristics of the specimens (e.g., number of vascular bundles, water content, etc.), all of the tested specimens demonstrated clear and significant time-dependent deformation under a constant load.

4. Discussion

This study used the sweet sorghum Della cultivar, which showed a minimal transition region between the rind and the pith and a relatively large region of pith (**Figure 1**). Its stems were significantly stiffer and stronger than the pith itself due to the presence of the rind (**Figure 2**). The rind is composed of high-density fiber bundles within the cell walls, which lead to stiffer and stronger tissues compared to the pith, which is composed of relatively weak thin-walled parenchyma cells and vascular bundles [31]. The non-dense/fibrous nature of the pith, as well as loss of water during compression, appeared to produce its highly nonlinear mechanical response (**Figure 2**). This nonlinear response has implications in lodging, which inherently involves large deformation beyond the linear elastic regime. We also surmise that the continuous straining (plateaus in stress in **Figure 2**) arose from morphological changes such as vascular bundle delamination from the parenchyma cells, and densification of parenchyma cells under mechanical loading. Compression of the specimens at high loads resulted in stiffening, likely due to densification of the cell walls at high strains, thereby requiring high loads to produce morphological changes upon further loading.

The compressive response of the Della stem indicated nonlinear behavior up to the peak stress, followed by softening, a large plateau in stress, and ultimately more stiffening toward the end of loading. The failure in the stem was associated with buckling and splitting of the rind layer from the pith and the softening was followed by water draining from the stem (**Figure 1b, Videos 1 and 3**). Splitting/buckling reduces the load carrying capability of the structures, particularly of the rind itself. Upon completion of buckling, further compressing the specimens stiffened the response, similar to that observed in the pith, and again likely resulted from densification of the cell walls. Different rates of uniaxial compression tests for both stem and pith showed the time-dependent nature of the sorghum structure (**Figure 2**). For both the pith and stem, the slower rate (10%/min) produced smaller peak stresses at larger corresponding strains due to more stress relaxation occurring during slower loading.

The effect of time-dependent behavior was further investigated by conducting creep tests on the Della pith and stem, which has further implications for rate dependent behavior. Della showed pronounced time-dependent behaviors during the creep tests. These responses indicated large permanent deformations which were likely associated with the morphological changes of pith tissues under mechanical loading, as evidenced by the pith itself exhibiting a more prevalent creep deformation than the full stem (rind and pith).

Thereafter, holding the load constant for about one hour showed that the pith exhibited a pronounced time-dependent response without additional water flowing out of the specimens, suggesting a viscoelastic mechanism.

As mentioned above, the time-dependent response of the tested piths was likely associated with a combination of poroelasticity and viscoelasticity. We attribute the poroelastic effect to the migration of water through the specimen and even out of the specimens under compression. Viscoelasticity also likely occurred due to the plant's composition of cellulose microfibrils and lignin matrices. Cellulose and lignin are long chain polymers with complex network microstructures. Some of time-dependent responses likely occurred due to reorientation of the microfibrils and macromolecular networks of the cellulose and lignin during loading. Viscoelastic effects were evidenced by a continuous increase in the strain when the load was kept constant (**Figure 3a**), even though no additional water was flowing out of the pith. However, we should note that in general, the viscous fluid flow of water within and through the cell walls (but not entirely out of the plant) might also contribute to the time-dependent response of the pith. Based on the current experimental data, it is difficult to separate the poroelastic and viscoelastic effects and determine the corresponding material parameters. However, the present study highlights the prevalence and importance of the time-dependent responses of sorghum.

Given the observed time-dependent behavior, simply using the 'elastic modulus' and treating the stems as elastic materials, as has been done in previous studies, will not provide enough information to fully capture sorghum's mechanical behavior under realistic loading conditions. Instead, time-dependent biomechanical models should be developed. Likewise, when the 'elastic modulus' is determined by quantifying the initial slope of the stress-strain curve, different values will be measured under different loading rates, as we have reported in comparing **Figures 2a and 2b**. Additionally, sorghum stems are naturally anisotropic, due to the axial orientation of fiber bundles. As such, different loading modes and directions, e.g., from complex loading from wind, will produce different mechanical responses. Specifically, we found average initial slopes of stems under axial compression of 130 MPa and 178 MPa, depending on the strain rate. These values are smaller than moduli measured by Lemloh et al. from bending tests (350 – 630 MPa) [27]. Another study reported the elastic modulus of sorghum stems in the transverse direction (using flat knives) of 4.6 – 13.2 MPa, which are much smaller than our measurements under axial compression [32]. We should note that these differences in values likely arise from more factors than simply the loading mode, including differences in genotype, stage of crop maturity, specific internode tested, and experimental testing setup. Future studies should consider detailed assessments of specific microstructural changes in sorghum that correspond to our macroscopically observed nonlinear time-dependent mechanical behavior. Finally, to our knowledge, time-dependent behaviors have not been explored in other grass stems, although several studies in other plants [33-36] seem to indicate that viscoelasticity occurs. We believe that

other cereal grass stems, particularly fresh (not dry) samples, will also show pronounced time-dependent behaviors that may be attributed to both poroelasticity and viscoelasticity, thereby motivating future studies.

5. Conclusions

To investigate the nonlinear and time-dependent responses of sweet sorghum stems, uniaxial compression and creep tests were conducted on the pith and stem of Della sorghum grown in a controlled environment in a greenhouse. The calculated initial slopes of the Della pith under uniaxial compression were 25.8 (± 8.0) MPa for slow loading (10%/min) and 36.4 (± 7.5) MPa for fast loading (100%/min). The corresponding slope of Della stems under uniaxial compression were 130.1 (± 30.1) MPa for slow loading (10%/min) and 177.9 (± 50.5) MPa for fast loading (100%/min). Beyond the linear region, under slow loading (10%/min), the pith showed a peak stress of 1.4 (± 0.5) MPa at a strain of 14.1 (± 6.7) %; under fast loading (100%/min), the pith showed a peak stress of 1.5 (± 0.3) MPa at a strain of 6.2 (± 1.4) %. Likewise, under slow loading (10%/min), the full stems showed a peak stress of 3.3 (± 0.3) MPa at a strain of 7.4 (± 1.8) %; under fast loading (100%/min), the stems showed a peak stress 4.0 (± 0.6) MPa at a strain of 5.9 (± 1.4) %. Both the pith and the stem exhibited highly nonlinear responses at larger strains: plateaus in stress, followed by stiffening at high compressive strains. All of these results indicate that Della sorghum exhibits pronounced rate/time-dependent biomechanical behavior. Creep tests further corroborated its significant time-dependent mechanical behavior, which we surmise arises from effects of both poroelasticity and viscoelasticity. Poroelastic effects were evidenced through the observed water loss in the sorghum pith during loading. Viscoelastic effects also likely arose due to the delayed responses of cellulose microfibrils and lignin matrices to mechanical loading, which lead to rearrangements of the macromolecular networks. Overall, this paper provides clear evidence of nonlinear and time-dependent biomechanical responses of sorghum piths and stems, which can guide more systematic studies aimed at understanding the mechanisms of the complex biomechanical responses of grass stems. Furthermore, this study provides several insights into the behavior of crops in the agricultural environment. It is possible that strong winds could result in creep responses and deformation of the stems of field grown plants, as a consequence of both poroelastic processes such as water migration and viscoelastic processes such as disruption of structural polymers. Such responses could contribute to stem failure (lodging) often observed in crops experiencing inclement weather.

Acknowledgments

This research is sponsored by the National Science Foundation under grant CMMI-1761015. The authors are thankful to Yuchen Shang for helping with sample preparation. We also thank Coleman Fincher for his advice on using a precision saw to cut the samples.

References

1. Shah, D.U., T.P. Reynolds, and M.H. Ramage, *The strength of plants: theory and experimental methods to measure the mechanical properties of stems*. Journal of experimental botany, 2017. **68**(16): p. 4497-4516.
2. Slewinski, T.L., *Non-structural carbohydrate partitioning in grass stems: a target to increase yield stability, stress tolerance, and biofuel production*. Journal of Experimental Botany, 2012. **63**(13): p. 4647-4670.
3. Berry, P., et al., *Understanding and reducing lodging in cereals*. Advances in Agronomy, 2004. **84**(04): p. 215-269.
4. Bashford, L., et al., *Mechanical properties affecting lodging of sorghum*. Transactions of the ASAE, 1976. **19**(5): p. 962-966.
5. Flint-Garcia, S.A., et al., *Quantitative trait locus analysis of stalk strength in four maize populations*. Crop Science, 2003b. **43**(1): p. 13-22.
6. Hu, H., et al., *QTL mapping of stalk bending strength in a recombinant inbred line maize population*. Theoretical applied genetics, 2013. **126**(9): p. 2257-2266.
7. Li, K., et al., *Genetic architecture of rind penetrometer resistance in two maize recombinant inbred line populations*. BMC plant biology, 2014. **14**(1): p. 152.
8. Mullet, J., et al., *Energy sorghum—a genetic model for the design of C4 grass bioenergy crops*. Journal of experimental botany, 2014. **65**(13): p. 3479-3489.
9. Pedersen, J.F. and J. Toy, *Measurement of sorghum stalk strength using the Missouri-Modified Electronic Rind Penetrometer*. Maydica, 1999. **44**: p. 155-158.
10. Peiffer, J.A., et al., *The genetic architecture of maize stalk strength*. Plos one, 2013. **8**(6): p. e67066.
11. Robertson, D., et al., *An improved method for accurate phenotyping of corn stalk strength*. Crop Science, 2014. **54**(5): p. 2038-2044.
12. Zuber, M. and C. Grogan, *A New Technique for Measuring Stalk Strength in Corn 1*. Crop Science, 1961. **1**(5): p. 378-380.
13. Robertson, D.J., et al., *Corn stalk lodging: a forensic engineering approach provides insights into failure patterns and mechanisms*. Crop Science, 2015a. **55**(6): p. 2833-2841.
14. Robertson, D.J., S.L. Smith, and D.D. Cook, *On measuring the bending strength of septate grass stems*. American journal of botany, 2015b. **102**(1): p. 5-11.
15. Dillon, S.L., et al., *Domestication to crop improvement: genetic resources for Sorghum and S accharum (Andropogoneae)*. Annals of botany, 2007. **100**(5): p. 975-989.
16. Doggett, H., Longman Scientific & Technical, 1988.
17. Doggett, H. and B. Majisu, *Disruptive selection in crop development*. Heredity, 1968. **23**(1): p. 1.
18. Harlan, J. and J. De Wet, *A Simplified Classification of Cultivated Sorghum 1*. Crop science, 1972. **12**(2): p. 172-176.
19. Flint-Garcia, S.A., et al., *Phenotypic versus marker-assisted selection for stalk strength and second-generation European corn borer resistance in maize*. Theoretical Applied Genetics, 2003a. **107**(7): p. 1331-1336.
20. Niklas, K.J., *Plant biomechanics: an engineering approach to plant form and function*. 1992: University of Chicago press.

21. Pinthus, M.J., *Estimate of genotypic value: A proposed method*. Euphytica, 1973. **22**(1): p. 121-123.
22. Gardiner, B., P. Berry, and B. Moulia, *Wind impacts on plant growth, mechanics and damage*. Plant Science, 2016. **245**: p. 94-118.
23. Speck, T. and I. Burgert, *Plant stems: functional design and mechanics*. Annual review of materials research, 2011. **41**: p. 169-193.
24. Gomez, F.E., et al., *High throughput phenotyping of morpho-anatomical stem properties using X-ray computed tomography in sorghum*. Plant methods, 2018. **14**(1): p. 59.
25. Gomez, F.E., et al., *Identifying morphological and mechanical traits associated with stem lodging in bioenergy sorghum (Sorghum bicolor)*. BioEnergy Research, 2017. **10**(3): p. 635-647.
26. Gomez, F.E., A.H. Muliana, and W.L. Rooney, *Predicting stem strength in diverse bioenergy sorghum genotypes*. Crop Science, 2018. **58**(2): p. 739-751.
27. Lemloh, M.-L., et al., *Structure-property relationships in mechanically stimulated Sorghum bicolor stalks*. Bioinspired Materials, 2014. **1**(1).
28. Berry, P., R. Sylvester-Bradley, and S. Berry, *Ideotype design for lodging-resistant wheat*. Euphytica, 2007. **154**(1-2): p. 165-179.
29. Kashiwagi, T., et al., *Improvement of lodging resistance with QTLs for stem diameter in rice (Oryza sativa L.)*. Theoretical and applied genetics, 2008. **117**(5): p. 749-757.
30. Wright, C.T., et al., *Biomechanics of wheat/barley straw and corn stover*. Applied biochemistry and biotechnology, 2005. **121**(1-3): p. 5-19.
31. Li, M., et al., *Physical fractionation of sweet sorghum and forage/energy sorghum for optimal processing in a biorefinery*. Industrial crops, 2018. **124**: p. 607-616.
32. Chattopadhyay, P. and K. Pandey, *Mechanical properties of sorghum stalk in relation to quasi-static deformation*. Journal of Agricultural Engineering Research, 1999. **73**(2): p. 199-206.
33. Brüchert, F., O. Speck, and H.C. Spatz, *Oscillations of plants' stems and their damping: theory and experimentation*. Philosophical Transactions of the Royal Society of London. Series B: Biological Sciences, 2003. **358**(1437): p. 1487-1492.
34. Hansen, S.L., et al., *Mechanical properties of plant cell walls probed by relaxation spectra*. Plant Physiology, 2011. **155**(1): p. 246-258.
35. Hayot, C.M., et al., *Viscoelastic properties of cell walls of single living plant cells determined by dynamic nanoindentation*. Journal of experimental botany, 2012. **63**(7): p. 2525-2540.
36. Spatz, H., L. Kohler, and K. Niklas, *Mechanical behaviour of plant tissues: composite materials or structures?* Journal of Experimental Biology, 1999. **202**(23): p. 3269-3272.

Figures

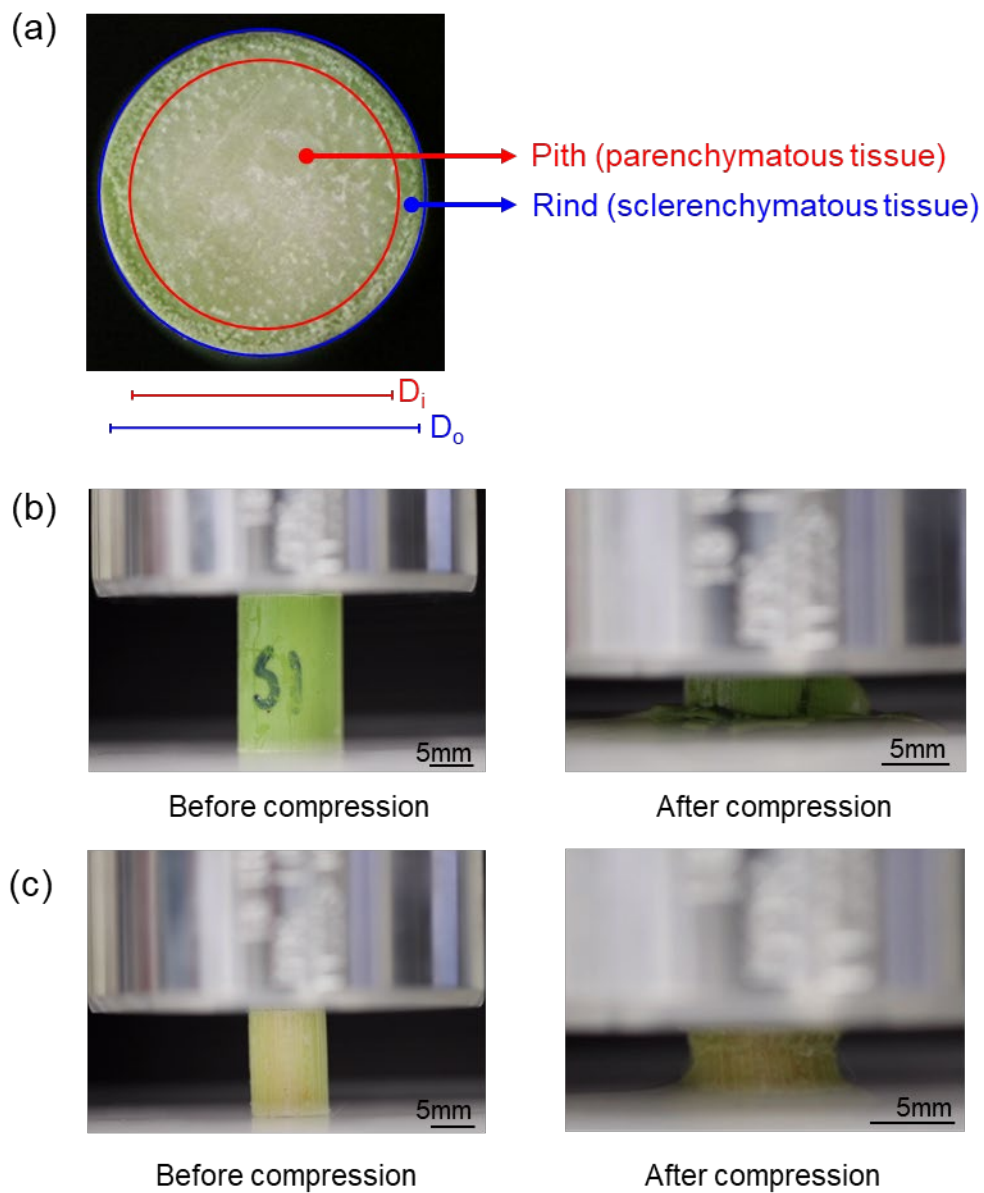


Figure 1. Representative photos of Della sweet sorghum. (a) Anatomical structure of a cross section of a Della stem. White dots correspond to vascular bundles. (b) Cross-section of a Della stem before and after compression testing. (c) Cross-section of a Della pith before and after compression testing.

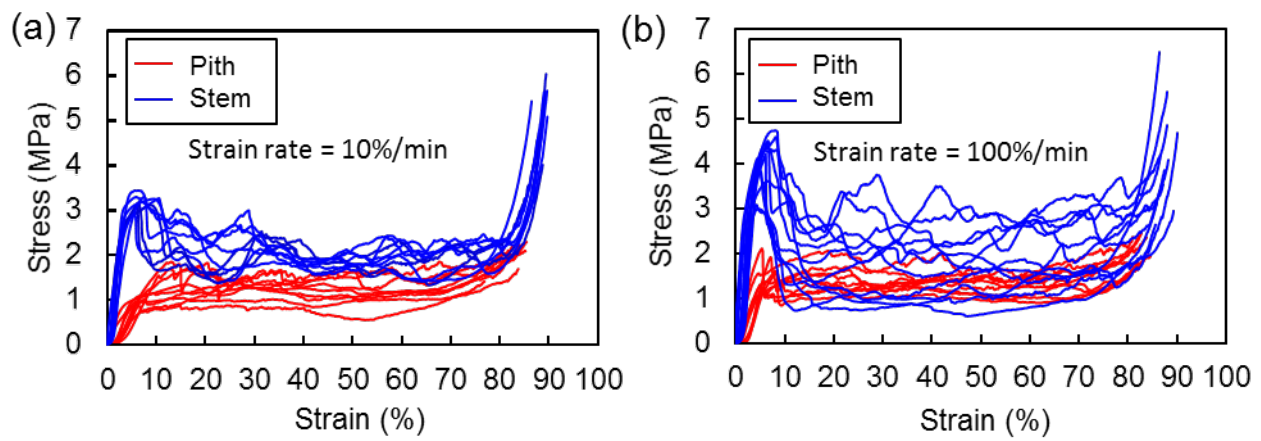


Figure 2. Stress-strain curves of uniaxial compression testing of Della pith and stems (a) at a strain rate of 10%/min (12 pith specimens and 10 stem specimens) and (b) at a strain rate of 100%/min (9 pith specimens and 11 stem specimens).

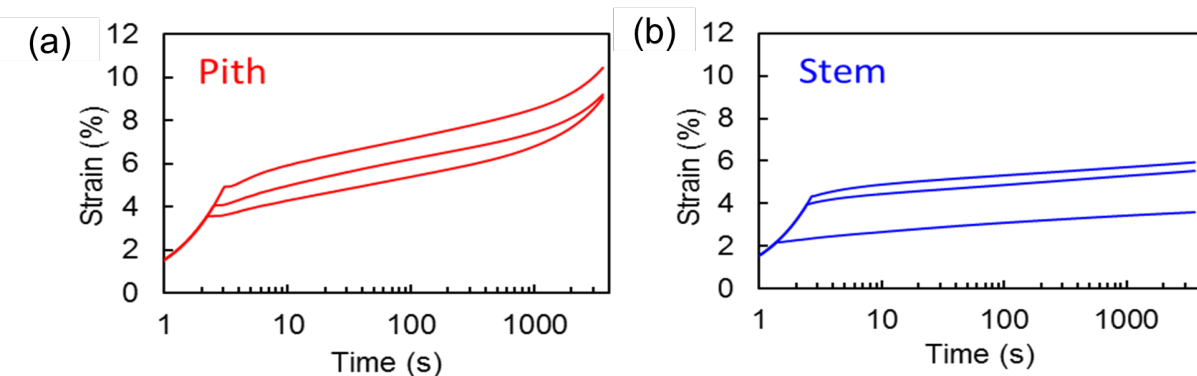


Figure 3. Creep tests: strain response during one hour under a static load. (a) Della pith (3 specimens) and (b) Della stem (3 specimens).

Tables

Table 1. Dimensions of Della piths tested under uniaxial compression with a strain rate of 10%/min. [Each specimen was taken randomly from internode 9 or 10 from among 10 replicate plants.](#)

| Uniaxial Compression of Piths (Strain Rate = 10%/min) | | | | |
|---|---------------|-------------|-------------------------|-----------------------|
| | Diameter (mm) | Height (mm) | Area (mm ²) | Diameter/Height Ratio |
| Pith 1 | 8.38 | 13.17 | 55.15 | 1.57 |
| Pith 2 | 8.69 | 9.96 | 59.31 | 1.15 |
| Pith 3 | 8.73 | 10.42 | 59.86 | 1.19 |
| Pith 4 | 8.86 | 10.44 | 61.65 | 1.18 |
| Pith 5 | 8.01 | 11.07 | 50.39 | 1.38 |
| Pith 6 | 7.95 | 11.28 | 49.64 | 1.42 |
| Pith 7 | 8.64 | 12.33 | 58.63 | 1.43 |
| Pith 8 | 8.06 | 11.54 | 51.02 | 1.43 |
| Pith 9 | 8.12 | 10.97 | 51.78 | 1.35 |
| Pith 10 | 8.64 | 12.38 | 58.63 | 1.43 |
| Pith 11 | 8.76 | 12.36 | 60.27 | 1.41 |
| Pith 12 | 8.61 | 12.52 | 58.22 | 1.45 |
| Average | 8.45 | 11.54 | 56.21 | 1.37 |
| Standard Dev | 0.33 | 1.01 | 4.363 | 0.13 |

Table 2. Dimensions of Della piths tested under uniaxial compression with a strain rate of 100%/min. [Each specimen was taken randomly from internode 9 or 10 from among 10 replicate plants.](#)

| Uniaxial Compression of Piths (Strain Rate = 100%/min) | | | | |
|--|---------------|-------------|-------------------------|-----------------------|
| | Diameter (mm) | Height (mm) | Area (mm ²) | Diameter/Height Ratio |
| Pith 1 | 8.15 | 11.72 | 52.17 | 1.44 |
| Pith 2 | 8.08 | 12.01 | 51.28 | 1.49 |
| Pith 3 | 8.77 | 11.98 | 60.41 | 1.37 |
| Pith 4 | 8.69 | 12.45 | 59.31 | 1.43 |
| Pith 5 | 7.36 | 11.77 | 42.54 | 1.6 |
| Pith 6 | 7.9 | 10.9 | 49.02 | 1.38 |
| Pith 7 | 8.64 | 11.69 | 58.63 | 1.35 |
| Pith 8 | 8.58 | 11.82 | 57.82 | 1.38 |
| Pith 9 | 8.77 | 11 | 60.41 | 1.25 |
| Average | 8.33 | 11.70 | 54.62 | 1.41 |

| | | | | |
|---------------------|------|------|------|------|
| Standard Dev | 0.49 | 0.49 | 6.22 | 0.10 |
|---------------------|------|------|------|------|

Table 3. Dimensions of Della stems tested under uniaxial compression with a strain rate of 10%/min. Each specimen was taken randomly from internode 9 or 10 from among 10 replicate plants.

Uniaxial Compression of Stems (Strain Rate = 10%/min)

| | Diameter (mm) | Height (mm) | Area (mm²) | Diameter/Height Ratio |
|---------------------|----------------------|--------------------|------------------------------|------------------------------|
| Stem 1 | 12.35 | 18.66 | 119.79 | 1.51 |
| Stem 2 | 12.58 | 18.31 | 124.29 | 1.46 |
| Stem 3 | 12.55 | 17.42 | 123.70 | 1.40 |
| Stem 4 | 12.74 | 19.24 | 127.48 | 1.51 |
| Stem 5 | 10.49 | 16.18 | 86.42 | 1.54 |
| Stem 6 | 11.78 | 17.42 | 108.99 | 1.48 |
| Stem 7 | 11.39 | 17.31 | 101.89 | 1.52 |
| Stem 8 | 11.59 | 18.83 | 105.50 | 1.62 |
| Stem 9 | 11.15 | 18.66 | 97.64 | 1.67 |
| Stem 10 | 11.38 | 18.04 | 101.71 | 1.59 |
| Average | 11.80 | 18.01 | 109.74 | 1.53 |
| Standard Dev | 0.74 | 0.92 | 13.57 | 0.08 |

Table 4. Dimensions of Della stems tested under uniaxial compression with a strain rate of 100%/min. Each specimen was taken randomly from internode 9 or 10 from among 10 replicate plants.

Uniaxial Compression of Stems (Strain Rate = 100%/min)

| | Diameter (mm) | Height (mm) | Area (mm²) | Diameter/Height Ratio |
|---------------------|----------------------|--------------------|------------------------------|------------------------------|
| Stem 1 | 11.42 | 17.38 | 102.43 | 1.52 |
| Stem 2 | 11.18 | 15.55 | 98.17 | 1.39 |
| Stem 3 | 11.03 | 15.15 | 95.55 | 1.37 |
| Stem 4 | 11.10 | 15.56 | 96.77 | 1.40 |
| Stem 5 | 12.21 | 19.93 | 117.09 | 1.63 |
| Stem 6 | 11.92 | 19.17 | 111.59 | 1.61 |
| Stem 7 | 10.42 | 13.91 | 85.27 | 1.34 |
| Stem 8 | 10.43 | 14.41 | 85.44 | 1.38 |
| Stem 9 | 10.69 | 16.76 | 89.75 | 1.57 |
| Stem 10 | 9.96 | 15.97 | 77.91 | 1.60 |
| Stem 11 | 10.84 | 15.95 | 92.29 | 1.47 |
| Average | 11.02 | 16.34 | 95.66 | 1.48 |
| Standard Dev | 0.66 | 1.86 | 11.58 | 0.11 |

Table 5. Dimensions of Della piths tested under compressive creep. Each sample was taken randomly from a plant among 10 replicates.

| Creep Tests of Piths | | | | |
|----------------------|---------------|-------------|-------------------------|-----------------------|
| | Diameter (mm) | Height (mm) | Area (mm ²) | Diameter/Height Ratio |
| Pith 1 | 10.53 | 14.10 | 87.09 | 1.34 |
| Pith 2 | 10.72 | 14.54 | 90.26 | 1.36 |
| Pith 3 | 10.74 | 13.15 | 90.59 | 1.22 |
| Average | 10.66 | 13.93 | 89.31 | 1.31 |
| Standard Dev | 0.12 | 0.71 | 1.93 | 0.07 |

Table 6. Dimensions of Della stems tested under compressive creep. Each sample was taken randomly from a plant among 10 replicates.

| Creep Tests of Stems | | | | |
|----------------------|---------------|-------------|-------------------------|-----------------------|
| | Diameter (mm) | Height (mm) | Area (mm ²) | Diameter/Height Ratio |
| Stem 1 | 11.61 | 18.50 | 105.86 | 1.59 |
| Stem 2 | 11.93 | 18.67 | 111.78 | 1.56 |
| Stem 3 | 12.14 | 18.55 | 115.75 | 1.53 |
| Average | 11.89 | 18.57 | 111.13 | 1.56 |
| Standard Dev | 0.27 | 0.09 | 4.97 | 0.03 |